

## Review Article

## Open Access

## Experimental HTSC-MAGLEV System and Efficiency Evaluation of a Noncontact Acceleration of IFE Target Placed in a Levitating Carrier

Irina Aleksandrova, Aleksandr Akunets, Sergei Gavrilkin, Olga Ivanenko, Evgeniy Koshelev, Kirill Mitsen, Andrei Nikitenko, Aleksei Tsvetkov and Elena Koresheva\*

P.N. Lebedev Physical Institute of Russian Academy of Sciences, Moscow, Russia

### ABSTRACT

Over the last two decades, superconducting materials have undergone an evolution that has broadened its application space. This work focuses on the issue of noncontact acceleration of fusion targets for fueling of a commercial Inertial Fusion Energy (IFE) power plant. This approach attracts a significant interest due to its potential for almost frictionless motion. The operational principle is the magnetic acceleration of the levitating target carrier (or HTSC-sabot) made from high-temperature superconducting tapes of the second generation (2G-HTSC). From physics, the possibility of their practical applications is directly related to the flux pinning of quantized magnetic flux lines in the superconductors (so called, high-pinning, Type-II HTSCs). The article describes the important achievements made in this area: 1) measurements of the magnetic moment of 2G-HTSC tapes ( $T_c = 92$  K) in the wide temperature range of 10–95 K; 2) building a circular PMG system (outer radius is  $R = 50$  mm,  $B = 0.13$ – $0.25$  T) to study magneto-thermo-mechanical interactions between HTSC-sabot and permanent magnets under external variable load with a rate of 2–5 Hz; 3) studying a static and dynamic stability of the guidance force for a set of different top-down suspended HTSC-sabots; 4) calculation of the HTSC-sabot velocity at which it leaves a circular trajectory at temperatures of  $\sim 80$  K to evaluate its behavior at  $T \sim 17$  K. The obtained results are in a good agreement that will allow one to estimate the parameters of a circular accelerator of  $R = 1$  m based on HTSC magnetic levitation (HTSC-MAGLEV) transport; the operating temperature is  $T \sim 17$  K which is characteristic of the target delivery to IFE power plant. The results of this work provide theoretical and experimental support for the practical design and application of such ac-celerator for reaching the target injection velocities in the range of 200–400 m/s.

### \*Corresponding author

Elena Koresheva, P.N. Lebedev Physical Institute of Russian Academy of Sciences, Moscow, Russia.

Received: May 19, 2023; Accepted: May 26, 2023; Published: June 01, 2023

**Keywords:** Inertial Fusion Energy, Cryogenic Fuel Target, Noncontact Target Delivery, High-Temperature Super-Conductors, HTSC-MAGLEV Technologies, Permanent Magnet Guideway.

### Introduction

One of the most important tasks in the field of the inertial fusion energy (IFE) is the creation of a system for the rep-rate delivery of free-standing cryogenic fusion targets (CFT) to the burn area of the high-power laser facility or IFE reactor [1]. The peculiarity of the delivery process lies in the requirements to the delivery rates (5–10 Hz), the accuracy of delivery and the temperature regime of delivery. The CFT must be positioned in the center of the reaction chamber with an accuracy of  $\pm 5$  mm. In this case, the accuracy of alignment of the laser beams and the CFT in the final position is  $\pm 20$   $\mu$ m. The spherical CFT (its diameter does not exceed 4 mm for a reactor class of CFTs) should have a temperature no higher than 18.3 K at the moment of its irradiation by a laser. The temperature of the reactor chamber wall itself can reach significant values (e.g., for the SOMBRERO reactor chamber, the indicated value is 1758 K [1]), and the overloads on the CFT during its acceleration in the injector can range from 5000  $\text{cm}^{-2}$  to 10000  $\text{cm}^{-2}$  [2].

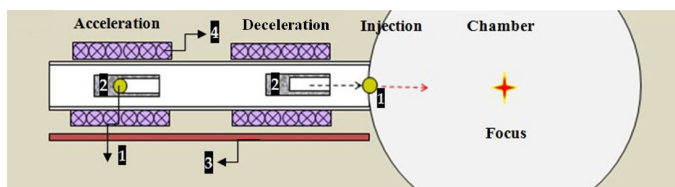
Other requirements to the delivery process are as follows:

- Targets must survive acceleration without damage, therefore, the acceleration of the CFT is carried out in a special carrier (or sabot), which transfers the moment of motion to the CFT;
- Targets must be accelerated to high injection speeds (200–400 m/s) to withstand the reaction chamber environment (thermal, gas, debris).
- Targets must remain highly symmetric, have a smooth inner surface of the D–T-ice layer, and must be at  $T = 18.3$  K before the laser shot to obtain the maximum energy yield from the fusion reaction.
- Targets must be placed into the accelerating medium operating at very low temperatures, allowing no heat energy to be passed into the CFT.

Note that the CFT acceleration technology is one of the key problems in the practical implementation of these requirements. Various traditional approaches for the CFT acceleration and injection are being studied in many IFE laboratories over the world. Among them are pneumatic and electromagnetic guns, electrostatic and gravity injectors. Regardless of the type of the CFT accelerator, for all of them there is a problem related to the

sabot friction against the wall of the injector guide tube, which can lead to a loss in the quality of the fuel layer. Note that according to, the maximum change in the temperature of the DT fuel inside the CFT should not exceed  $\sim 100$  mK. In addition, there is a risk of malfunction of the injector due to wedging of the sabot in the guide tube [4,5]. However, traditional approaches are useful for initial demonstrations, but in the long term, a noncontact accelerator is required that overcomes friction and demonstrates more efficient use of energy of motion.

Thus, the creation of a noncontact positioning and transport system for CFT is one of the most important tasks in the IFE program. Researches in this area carried out at the Lebedev Physical Institute of Russian Academy of Sciences (LPI) are based on the effect of quantum levitation of HTSCs in a magnetic field (Figure 1a). Main principles, material options and demonstration models for a noncontact acceleration of IFE targets using HTSC-MAGLEV systems are discussed in detail in [6]. A special emphasis was paid to creation of different PMG systems (or magnetic tracks), linear or circular ones. Additionally, we used high-pinning, Type-II HTSCs as a material for the CFT sabot (everywhere further HTSC-sabot) to completely exclude the contact of the sabot with the accelerator guide tube, i.e. to realize the HTSC-sabot movement without mechanical friction, i.e. in the absence of heat generated by friction.



(a)



(b)

**Figure 1:** HTSC-MAGLEV linear accelerator. In (a): schematic diagram of the main processes during the target delivery to the laser focus (top view, not to scale: 1 – target, 2 – HTSC-sabot, 3 – magnetic track, 4 – field coils); in (b): experimental modeling of the acceleration stage at  $T \sim 80$  K.

It should be noted that for IFF it is of great importance that such HTSC-MAGLEV transport can provide quick acceleration (“HTSC-sabot + CFT” gradually gains its velocity) and deceleration (stage of CFT separation from HTSC-sabot) at very high velocities [7]. For this reason, our work covers the activities related to a study of different permanent magnet guideway (PMG) building options to realize high running velocities in a limited PMG for optimizing both suspension and levitation of CFT placed in the HTSC-sabot.

Previously, we have demonstrated several possibilities of constructing an HTSC-MAGLEV linear accelerator for implementing noncontact delivery of CFTs to the focus of

a high-power laser facility [8]. The main elements of such an accelerator are the linear PMG-system, HTSC-sabot and the propulsion system, which includes a set of field coils to generate magnetic travelling waves those act on the HTSC-sabot. Since any superconductors are diamagnetic, they are pushed out of the region of a strong magnetic field, and therefore the HTSC-sabot was accelerated under the influence of a magnetic pulse (Figure 1b).

The results of experimental and theoretical modeling showed that a linear accelerator can be built for the entire range of injection velocities (200–400 m/s), moreover, for the maximum velocity  $v_{inj} = 400$  m/s, the acceleration length will be  $L_a = 20$  m at overloads  $a < 5000$  m/s<sup>2</sup>. If CFTs have sufficient mechanical strength, then another acceleration scenario can be realized:  $v_{inj} = 400$  m/s,  $L_a = 10$  m,  $a = 8000$  m/s<sup>2</sup> (which is less than the maximum allowable acceleration imposed on the target must be no higher than 10000 m/s<sup>2</sup>) [4]. Note that the linear accelerator is characterized by a significant number of the field coils (more than 100 pieces) to implement the acceleration process using a traveling magnetic wave.

At the moment, the LPI is successfully conducting researches on creation of the HTSC-MAGLEV systems for operation not only in the linear acceleration schemes, but also in different curved-line limited PMG-systems for realizing a cyclotron acceleration method [6]. This is very promising for reducing the size of the accelerator, as well as the number of the field coils to 2–4 pieces. The basic principles of constructing the limited PMG-systems were studied and the first successful experiments were carried out. In particular, when using only one field coil in an oval-shaped PMG (its size: major axis is 22 cm, minor axis is 9.5 cm) consisting of two linear and two curved parts, the velocity of the HTSC-sabot was  $\sim 1$  m/s for one turn (experiments were carried out at  $T \sim 80$  K).

This article presents the results of an experimental study of the HTSC-sabot acceleration above the circular PMG-system under creating an external variable load with an oscillation frequency of 2–5 Hz. Using measurements of the velocity, acceleration, and temperature characteristics of the 2G-HTSC tapes in various magnetic fields, we have studied the dynamic stability of the HTSC-sabot during its acceleration with the aim, in the future, to move from the mock-up experiments at  $T \sim 80$  K to the practical usage of such circular PMGs for CFT delivery at the laser focus – creation of a prototype of the HTSC-MAGLEV circular accelerator operating at  $T \sim 17$  K.

## Preparation of the Experiment

### Measuring the magnetic moment of the 2G-HTSC tapes

From physics, the possibility of the 2G-HTSC tapes practical applications is directly related to the flux pinning of quantized magnetic flux lines in the HTSCs [9-11]. Below the temperature  $T_C$  of superconducting state transition (Figure 2), the HTSCs are the materials which exhibit two superconducting states in applied magnetic fields ( $B$ ) and have therefore two critical magnetic fields  $B_{C1}$  and  $B_{C2}$ . The first is a state of perfect diamagnetism (due to Meissner effect, Figure 2b at  $B < B_{C1}$ ) when magnetic fields are expelled from the superconductor interior by the formation of surface currents. They penetrate the surface to a small extent. The penetration depths are typically in the range of 10–100 nm.

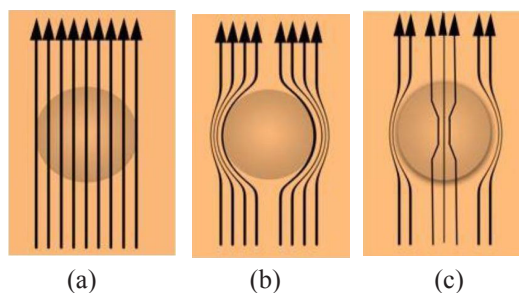


**Figure 2:** Under certain conditions the HTSCs permit a small amount of magnetic field to penetrate their bulk via filament-like vortices holding quantized magnetic flux. In (a):  $T > T_c$  is the normal state; in (b):  $T < T_c$  and  $B < B_{c1}$  is the Meissner state; in (c):  $T < T_c$  and  $B_{c1} < B < B_{c2}$  is the Abrikosov state (or mixed state).

However, if the value of  $B$  is increased ( $B > B_{c1}$ ), a transition to a second state occurs that allows the magnetic flux lines penetration through the HTSCs bulk. Thus, when the applied field  $B$  is between  $B_{c1} < B < B_{c2}$  (Figure 2c), the magnetic field is not excluded completely, but is constrained in filaments within the HTSCs. These filaments are in the normal state (Figure 2a) surrounded by super currents which are associated with a regular array of super current vortices, or a vortex lattice. This state is called the mixed or Abrikosov state [11]. The effect of capturing or pinning vortices in real HTSCs has essential meaning from the point of view of lateral levitation stability. Here, some remarks concerning the HTSCs properties are necessary.

The basic magneto-mechanical phenomenon responsible for stable levitation in the HTSC-maglev systems relies on the diamagnetic and magnetic flux pinning characteristics of the HTSC bulk in a magnetic field. In the mixed state (Figure 2c) the flux lines interact with different defects and may become pinned to them. Such defects (e.g., crystal lattice defects, grain boundaries, twin planes, stacking faults, etc.) always exist in real superconducting materials. They could work as pinning centers (including pinning by surface roughness or at a step-like surface relief) for avoiding the vortex motion. A vortex state looks like a "frozen vortex lattice" or "frozen magnetic field" in the HTSC bulk, and any spatial displacement of the superconductor will cause this "frozen magnetic field" to move. In order to prevent the vortex motion the superconductor remains "trapped" in its original state (be it levitation in the fixed space point or motion along a magnetic track). Thus, for transport applications it is important to search for materials with high pinning forces to enable sufficient levitation and guidance forces, and stability. Note that different ways on enhancement of superconducting properties and flux pinning mechanism are widely developed [12-14].

Regarding the role of the PMG scheme, we will address this issue below in Section 2.2 including the principle of the HTSC-sabot acceleration which is of great importance, both in the scientific and technological points of view.

Our study has shown that high-pinning 2G-HTSC tapes produced by SuperOx can be successfully used in the levitation experiments [14]. These are the SuperOx J-PI-12-20Ag-20Cu tapes of the following composition: Ag (2  $\mu\text{m}$ ), Cu (20  $\mu\text{m}$ ), a Hastelloy alloy substrate, C-276 (60  $\mu\text{m}$ ), non-magnetic. Their magnetic moment measurements were carried out using the multifunctional automated complex PPMS-9 (Quantum Design, Ltd) having the

following characteristics:

- The complex provides options to measure the magnetic moment,  $M$ , both in static and dynamic modes with an accuracy of  $\pm 2.5 \cdot 10^{-8} \text{ A}^2 \text{ m}^2$ .
- The temperature range available for measurement is 0.35–400.00 K with a temperature control no worse than 0.01 K.
- The range of the magnetic field available for measurements is  $\pm 9 \text{ T}$  with a field uniformity of no worse than 0.01%.

The temperature dependence of the magnetic moment of the 2G-HTSC tapes ( $M = \chi \cdot H$  where  $H$  is the magnetic field strength and  $\chi$  is the magnetic susceptibility of the HTSC sample) in various magnetic fields was measured in the zero-field cooled (ZFC) mode. When implementing the ZFC mode, a segment of the 2G-HTSC tape was cooled down to 10 K. After that a constant magnetic field was turned on, and the temperature slowly increased to the critical temperature  $T_c$  of the superconducting transition and higher (in our case  $T_c = 92 \text{ K}$ ). The measurements were carried out in the magnetic fields of 0.01; 0.5; 1.0; 2.0; 4.0; and 8.0 T. The number of measurements is about 1600 temperature points for each value of the magnetic field.

**Table 1: Characteristics of the 2G-HTSC tapes used in the levitation experiments**

HTSC	$\rho$ , g/cm <sup>3</sup>	$I_c$ , A at 7 K	$B_c$ , T at 0 K	$T_c$ , K
SuperOx, Ltd.	3.25	150	> 45	92

\*/ $\rho$  is the density of the 2G-HTSC tape,  $I_c$ ,  $B_c$ ,  $T_c$ , are the critical current, magnetic field and temperature.

The obtained measurement data in the temperature range of 10–85 K and the magnetic fields in the range of 0.5–8.0 T are shown in Figure 3.

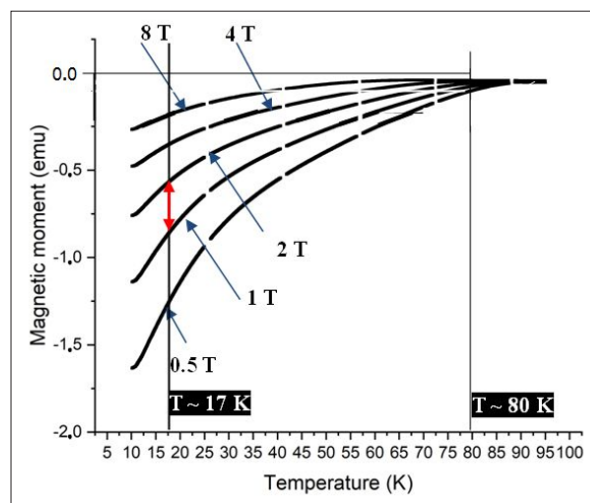


**Figure 3:** The results of measuring the magnetic moment (1 emu =  $10^{-3} \text{ A} \cdot \text{m}^2$ ) of the 2G-HTSC-tape using the automated complex PPMS-9:  $T \sim 80 \text{ K}$  is the temperature of experimental modeling of the acceleration stage;  $T \sim 17 \text{ K}$  is the temperature of CFT acceleration during its delivery at the laser focus.

The data for the magnetic fields of practical interest ( $B = 1 \text{ T}$  and  $B = 2 \text{ T}$ ) are summarized in Table 2. For the assembly "HTSC-sabot + CFT" to remain viable, such magnetic fields of the PMG will provide protection for a limited period during which it must complete its travel to the reaction chamber (Figure 1a).

**Table 2:** Measured values of the modulus of the magnetic moment  $|M|$  for a piece of the 2G-HTSC-tape manufactured by SuperOx (external field  $B = 1$  T and  $B = 2$  T).

T (K)	$ M $ , emu (B = 1 T)	$ M $ , emu (B = 2 T)
10	1.14022	0.75999
17	0.88404	0.58325
18	0.83826	0.55392
20	0.78202	0.51457
80	0.02	0.00209
83	0.00772	0.00269
85	0.00214	0.00384

\*/ a piece of 2G-HTSC tape was used with dimensions  $(4 \times 4)$  mm<sup>2</sup> and thickness 120 microns

The HTSC-MAGLEV accelerator must operate at a very low temperature ( $\sim 17$  K, see (Figure 3)). Important for the further discussion is the fact that the modulus  $M$  ( $|M|$ ) increases by 1–2 orders of magnitude depending on the value of the magnetic field as the operating temperature decreases from 85 K to 17 K. In particular, at  $B = 1$  T, when the operating temperature changes from 80 K to 17 K, the modulus of the magnetic moment increases in 44 times, when the temperature decreases from 83 K to 17 K, it increases in 114 times, and when the temperature decreases from 85 K to 17 K – in 413 times.

### Building a circular PMG-system

Here let us do several remarks about the principle of the HTSC-sabot acceleration. The main idea is a special PMG construction in which the magnetic field of PMG must allow the HTSC-sabot to move freely only in one direction (along the symmetry lines in the magnetic field distribution where the field gradient is zero (see formula (1) in Section 3) and produce a considerably strong gradient for a side-to-side motion in the cross section of the PMG. In other words, since HTSCs are diamagnetic, then the HTSC-sabot is pushed out from a stronger magnetic field and it returns to its original trajectory. The PMG building is the most critical issue of practical interest since it serves as the continuous magnetic track to generate the magnetic field by the rare-earth magnets. Its distribution in cross section causes levitation and guidance forces due to the pinning of flux lines in the HTSCs [9-11].

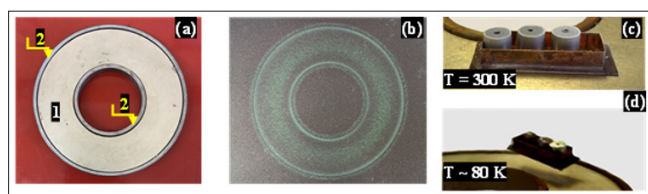


**Figure 4:** A circular PMG-system: (a) top view (1 is the magnet, 2 is the iron pot); (b) magnetic field mapping just on the PMG surface obtained by using the MFV-film; (c) HTSC-sabot with a load capacity of 3 cylindrical surrogate targets of  $\sim 1$  g each; (d) stable levitation of the HTSC-sabot over the PMG.

A circular PMG-system (Figure 4a) used in this work includes a ring magnet (1) fixed inside an iron pot (2). The latter guides and concentrates the magnetic flux onto the working PMG surface for creating the required magnetic field gradient (so-called "magnetic wall") for a stable levitation of the HTSC-sabot with increased load capacity (Figure 4c and 4d). Figure 4b shows the configuration of the magnetic field obtained using a magnetic field

viewing (MFV) film, which allows one to easily map the magnetic fields and directional patterns on the surface of any magnet or magnetic assembly. The MFV-film is a thin, translucent, flexible sheet coated with microcells filled with nickel particles in oil which align themselves along magnetic field lines. When the magnetic field lines are parallel to the surface of the MFV-film, the nickel particles turn their reflective side and appear light-colored areas. On a magnet pole, the magnetic field lines emerging from this pole pass through the film almost perpendicular to its surface, so it is dark in this place.

The characteristics of the permanent magnets composing the PMG-system are very important in terms of levitation force and stability:

- Disk magnet (made at Midora, Ltd.): made from NdFeB alloy with anticorrosion coating (Ni-Cu-Ni), size of the magnet – OD = 100 mm, ID = 50 mm, thickness is 5 mm; axial magnetic induction  $B = 0.13$ – $0.25$  T, weight is 218 g.
- Iron pot (made at LPI): soft magnetic iron ARMCO, OD = 105 mm, ID = 45 mm, height is 7.5 mm; depth of the chute for the magnet is 5 mm.
- HTSC used in the experiments can operate above 77 K, the boiling point of liquid nitrogen, because its  $T_C = 92$  K.

As we have seen from Figure 4b, the PMG magnetic field has a circular symmetry. This means that the magnetic flux does not change along the circular tracks allowing the HTSC-sabot to move around them. In all other directions, its movement will be blocked in order to avoid any contact with a stronger magnetic field.

Figure 5: shows a magnetic field distribution at different heights,  $h$ , over the PMG surface. The measurements were performed with an MF-1 NOVOTEST magnetometer based on a DKhK-0.5A Hall sensor with a sensitivity of 280 mV/T. Measurement range  $\pm 250$  mT, absolute error  $\pm 5$  mT, sensing element positioning accuracy 0.1 mm.

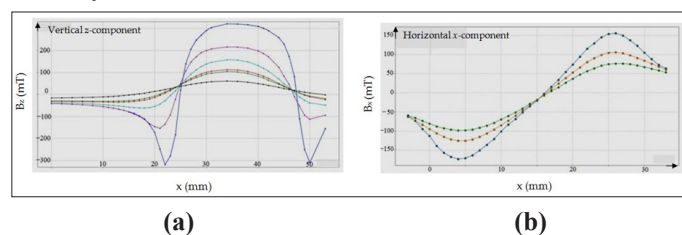


**Figure 5:** The results of measuring the magnetic field of the circular PMG-system: (a) the vertical z-component ( $B_z$ ) at different heights: blue corresponds to  $h = 1$  mm, purple corresponds to  $h = 4$  mm, aquamarine corresponds to  $h = 7$  mm, red corresponds to  $h = 10$  mm, green corresponds to  $h = 11$  mm, black corresponds to  $h = 16.5$  mm; (b) horizontal x-component ( $B_x$  along the x-direction): blue corresponds to  $h = 6$  mm, orange corresponds to  $h = 8$  mm, green corresponds to  $h = 10$  mm.

For the present study, we used two simplest mock-ups made from 2G-HTSC tapes (see Table 1) surrogating the HTSC-sabots in the form of a "trough" mounted on the substrate (Sabot #1) and a "hollow parallelepiped" (Sabot #2). They are shown in Figure 6.

Note that the sabot weights are 1.25 g and 1 g that is significantly less than that of a reactor CTF  $\sim 4.5$  mg, i.e. the CTF does not affect the load capacity of both HTSC-sabots [2]. The experiments were carried out at  $T \sim 80$  K  $< T_C = 92$  K. To avoid rapid back-heating of the HTSC-sabots, simple insulating materials and some

combinations of them are usually used: aluminum foil, liquid nitrogen (Figure 6b, boiling point of liquid nitrogen is 77 K), or polymer foam saturated with liquid nitrogen (Figure 6d, hollow parallelepiped with open ends and foam filler), which makes the required quantity of refrigerant is the main operational cost.

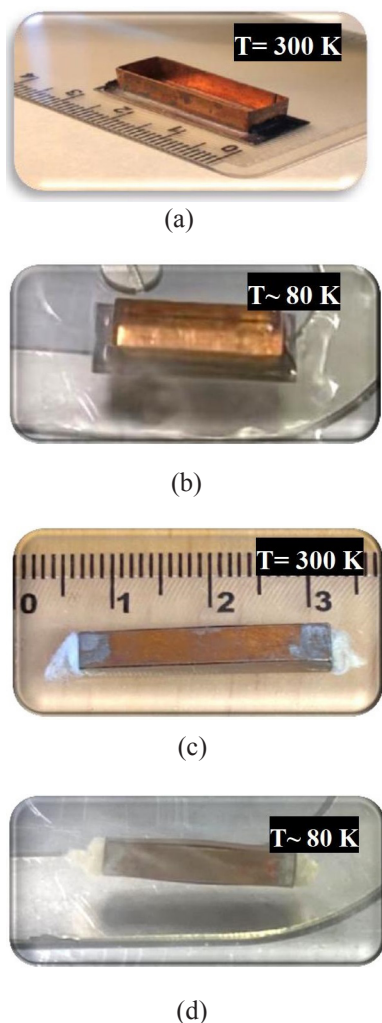


**Figure 6:** Two HTSC-sabot mockups: (a, b) Sabot #1, (its parameters are the following: substrate dimensions are equal to  $(30 \times 12) \text{ mm}^2$ , thickness is 0.2 mm; trough dimensions is length 8 mm, width 5 mm, height 4 mm; total weight 1.25 g); (c, d) Sabot #2 (its parameters are the following: dimensions are equal to  $(4 \times 4 \times 24) \text{ mm}^3$ , wall thickness is 1 mm; total weight is 0.97 g).

Before the placement of these HTSC-sabots over the circular PMG-system, we have used the ZFC process which is commonly applied to prepare the objects for studding the running performance of the magnetic levitation track. A feature of this process is that it is carried out by cooling the superconductors in the absence of a magnetic field.

### Results of Experimental and Theoretical Modelling

We have started a new series of the experiments to study the motion of both HTSC-sabots over the circular PMG-system with an increasing velocity along the trajectory like a “unwinding helix”. A setup to change the slope angle  $\alpha$  of the track is shown in Figure 7a, and a corresponding schematic diagram is shown in Figure 7b.



**Figure 7:** Experimental setup: (a) general view, (b) schematic diagram for creating EVL with an oscillation frequency in the range of 2–5 Hz (1 is the Styrofoam as a fit bed for the PMG, 2 is the cylinder of 7-mm diameter).

The procedure looks as follows:

- Cool the HTSC-sabot in liquid nitrogen;
- Place the cooled HTSC-sabot above the PMG track;
- Change the slope angle of the track by changing the plane of the Styrofoam bath-holder.

An external variable load (EVL) is generated due to changing the inclination angle  $\alpha$  and has two components:

- Normal to the PMG surface ( $F_{\perp} = mg \cdot \cos\alpha$ ) to balance the levitation force;
- Parallel to the PMG surface ( $F_{\parallel} = mg \cdot \sin\alpha$ ) to initiate the HTSC-sabot motion along the circular PMG.

Initially, in the experiments we used Sabot #2. The angle  $\alpha$  was changed from  $3.3^\circ$  to  $0^\circ$  with a frequency of 2–5 Hz. The sabot was placed above the PMG track and set in motion under the EVL due to changing the angle  $\alpha$  of the bed to the beat of the HTSC-sabot rotation.

Our work has centered on modeling a cyclotron acceleration process under increasing impact on Sabot #2. As seen from Figure 8, Sabot #2 gradually picks up its velocity and begins going away from the center of the circular PMG track due to the centrifugal force. In frames 1–4: 1st turn – Sabot #2 moves along the inner diameter; in frame 5: 2nd turn – slow drift away from the inner diameter; in frames 6–8: 10th turn – upon reaching a certain velocity of “stall” (which depends on the magnitude and configuration of the magnetic field), Sabot #2 leaves the magnetic track (frames 7 and 8).

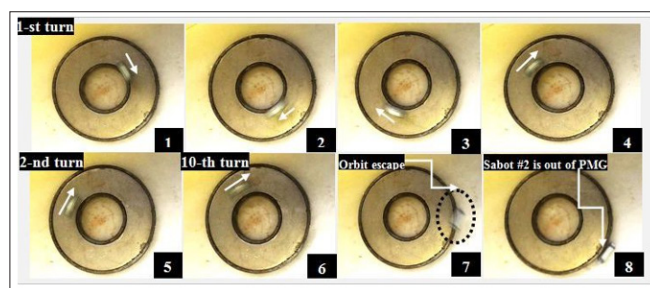


**Figure 8:** Freeze frames of Sabot #2 movement at  $h = 8 \text{ mm}$  over the circular PMG with an increasing velocity, and when a certain value is reached ( $v_{out} = 0.6 \text{ m/s}$ ), it tangentially leaves the trajectory.

We emphasize that the magnetic field of the PMG plays the role of a “magnetic wall” that holds the HTSC-sabot inside the track until its kinetic energy exceeds the energy of interaction with the magnetic field. More specifically, the value of a “stall” velocity,  $v_{out}$ , is determined by the parameters of used HTSC material and PMG-system (magnetic moment  $|M|$  and the magnetic force field along the x-direction  $K_x = B_x(dB_x/dx)$ ), and the more the value of  $|M|$ , the smaller  $K_x$  is required to maintain a required HTSC-sabot velocity.

Let us estimate the value of  $v_{out}$  based on the measurements performed in this work (see Figures 3 and 5). The force  $F_x$  acting on the HTSC-sabot in the  $x$ -direction (in our case along the PMG radius) caused by the coupled-action of the magnetization and magnetic field gradient, can be expressed by the following equation [10]:

$$F_x = (\chi/2\mu_0)V_s(\partial B^2/\partial x), \quad (1)$$

Where  $\mu_0$  is the vacuum permeability,  $\chi$  is the magnetic susceptibility of the HTSC material,  $V_s$  is the sabot volume, and  $B$  is the magnetic induction. To determine  $\chi$ , the magnetic moment  $M = \chi \cdot H$  was measured in the ZFC mode using the PPMS-9 complex (see Section 2.1).

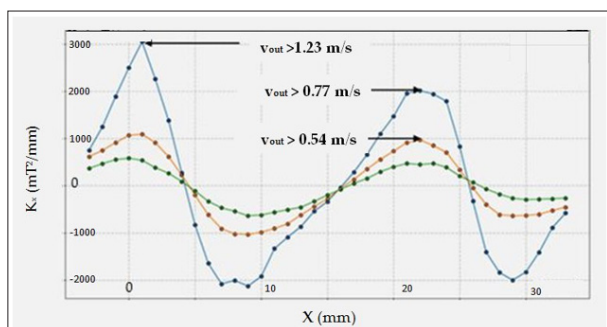
When moving in a circle, the HTSC-sabot interacts with the PMG field (parameters in Figure 5), creating a force  $F_x$  to balance the centrifugal force  $F_c = mv^2/R$ , where  $m$  is the sabot mass,  $v$  is its velocity,  $R$  is the radius of the circular trajectory. Using formula (1) and the results obtained in [6], the mechanical equilibrium equation of the HTSC-sabot running stably over the circular PMG can be written as:

$$K_x = B_x (dB_x/dx) = \mu_0\eta(v^2/R), \quad (2)$$

Where the parameter  $\eta$  characterizes the properties of the HTSC materials:  $\eta = \rho/\chi$ , where  $\rho = m/V_s$ .



(a)



(b)

**Figure 9:** The stall velocities of the HTSC-sabot moving at different levitation heights over the circular PMG. In (a): magnetic field measurements by the magnetometer with a positioning accuracy of 0.1 mm; in (b): stall velocities as a function of the magnetic force field  $K_x = B_x(dB_x/dx)$  for several levitation heights: blue corresponds to  $h = 6$  mm, orange corresponds to  $h = 8$  mm, green corresponds to  $h = 10$  mm. The calculation parameters are as follows: HTSC density is  $\rho = 3.25$  g/cm<sup>3</sup>,  $|M| = 0.03$  emu at  $T = 82$  K,  $\eta = 1.04 \cdot 10^3$  g/cm<sup>3</sup>, the  $x$ -axis goes from the outer edge of the PMG (see Figure 9a).

The values of  $\eta$  and  $R$  will determine the most important characteristics of the PMG-system (intensity and distribution of its magnetic field) along the  $x$ -direction for each individual

velocity  $v$ . The measurement procedure is shown in Figure 9a. The calculation results for the experimentally measured value of  $K_x$  related to our PMG-system are shown in Figure 9b.

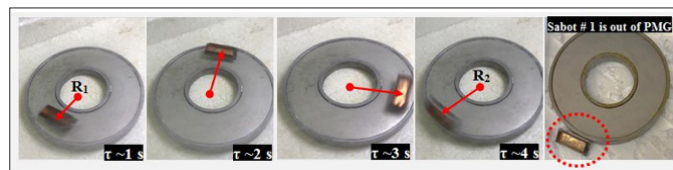


**Figure 10:** Freeze frames of Sabot #1 movement at  $h = 6$  mm at different times (frames 1–4): at R1 Sabot #1 starts its rotation; at R2 Sabot #1 flips over and leaves the track when its velocity becomes equal to  $v_{out} = 1.32$  m/s. The last frame shows Sabot #1 after its stall from the trajectory.

They are in good agreement with the experimental studies (Figures 8 and 10). From the experimental and calculated results above mentioned, for  $K_x = 1000$  mT<sup>2</sup>/mm and levitation height  $h = 8$  mm the stall velocity is  $v_{out} > 0.54$  m/s, and the HTSC-sabot tangentially leaves the circular trajectory practically in the middle of the track at  $v_{out} = 0.6$  m/s (see Figure 8); for  $K_x = 3000$  mT<sup>2</sup>/mm and  $h = 6$  mm the stall velocity is  $v_{out} = 1.32$  m/s, and the HTSC-sabot tangentially leaves the trajectory along the outer diameter of the PMG-system (see Figure 10).

### Discussion of the Obtained Results

Consider the possibility of transition from mock-up experiments to creation of a prototype of the circular accelerator for the system of noncontact delivery of CFT to the ICF chamber. To do this, let us estimate the value of the injection velocity, which can be realized with the help of such an accelerator. Using relation (2), this velocity can be written as:

$$v = (K_x R / (\mu_0 \eta))^{1/2} \quad (3)$$

From (5) it follows that for a given radius of the circular PMG-system, the greater the velocity, the smaller the parameter  $\eta$  and the greater the value of  $K_x$ . To carry out the estimates, we take into account the following important aspects:

1) In strong magnetic fields ( $B \sim 2-3$  T), the required gradients  $\sim 5 \cdot 10^2$  T<sup>2</sup>/m can be realized at very short distances, which limits the size of accelerated two bodies to values of the order of centimeters. Since the diameter of the reactor CFT does not exceed 4 mm [2], this condition can be easily implemented in practice when constructing the cycling accelerator.

2) The technological progress in the improvement of the quality parameters and the shapes of HTSCs has opened a wide range of possible applications of these materials. At present, HTSCs with unique properties are being synthesized. For example, several groups of porous superconductors with a low density have been studied. The pores in such materials ensure the penetration of coolant, efficient heat dissipation and stable operation of the levitation system. A review of research on superconductors with a porosity of more than 50% is presented in [15]. These data indicate the possibility of reducing the value of  $\eta$  due to a decrease in the density of HTSCs used to fabricate superconducting CFT carriers.

3) Additionally, take into account the fact that the CFT accelerator must operate at sufficiently low temperatures  $\sim 17$  K. Measurements of the magnetic moment of 2G-HTSC tape (see Section 1) have showed that the value of  $|M|$  increases by more than 2 orders of magnitude as its temperature decreases from 85 K to 17 K for the

magnetic fields we are interested in ( $B \sim 1-2$  T).

Let us make estimations for a cyclotron accelerator with  $R = 1$  m,  $K_x = 500$  T<sup>2</sup>/m (which can be written as  $K_x = 2T \times 0.25$  T/mm) and the value of  $|M|$  only an order of magnitude greater than in our experiments at  $T \sim 80$  K. In this case, the stall velocity according to relation (3) will be  $v_{out} \sim 220$  m/s. Further improvement of the accelerator scheme (a combination of linear and circular tracks in the construction of the magnetic system, as well as the choice of promising HTSC materials, allows us to conclude that the realization of the required injection rates of 200–400 m/s is possible.

### Conclusion

The experimental and theoretical modeling carried out in this work has shown that the ability of CFT to withstand the thermal and mechanical overloads during its delivery to the reactor chamber can be successfully solved using a new type of accelerator – HTSC-MAGLEV in a linear or circular modification with a cyclotron acceleration mode. The advantage here is the noncontact transport and therefore the absence of wear and mechanical friction. As a result, the issue of de-veloping the cryogenic lubricants is removed, the effectiveness of which at cryogenic temperatures ( $T < 20$  K) is highly questionable. All this improves efficiency and reduces maintenance costs, which prolongs the service life of the CFT delivery system, especially when it operates under conditions of CFT injection into the reactor chamber at the required rate of 5–10 Hz.

**Author Contributions:** “Conceptualization, Irina Aleksandrova and Elena Koresheva; methodology, Olga Ivanenko, Kirill Mitsen; software, Andrei Nikitenko; validation, Elena Koresheva and Andrei Nikitenko; for-mal analysis, Irina Aleksandrova; investigation, Irina Aleksandrova, Aleksandr Akunets, Sergei Gavrilkin, Evgeniy Koshelev, Elena Koresheva and Aleksei Tsvetkov; resources, Aleksandr Akunets; data curation, Irina Aleksandrova; writing—original draft preparation, Irina Aleksandrova; writing—review and editing, Elena Koresheva; project administration, Elena Koresheva; funding acquisition, Elena Koresheva. All authors have read and agreed to the published version of the manuscript.

**Funding:** This research was funded by IAEA, grant number 24154 and by the LPI State Task 4

**Conflicts of Interest:** The authors declare no conflict of interest.

### References

1. Goodin DT, Alexander NB, Besenbruch GE, Bozek AS, Brown LC, et al. (2006) Developing a commercial production process for 500000 targets per day: A key challenge for inertial fusion energy. *Phys Plasmas* 13: 1-4.
2. Bodner SE, Colombant DG, Schmitt AJ, Klapisch M (2000) High Gain Target Design for Laser Fusion. *Phys Plasmas* 7: 2298-2301.
3. Goodin DT, Alexander NB, Brown LC, Frey DT, Gallix R, et al. (2004) A cost-effective target supply for inertial fusion energy. *Nucl Fusion* 44: S254-S265.
4. Miles R, Spaeth M, Manes K, Peter Amendt, Max T, et al. (2011) Challenges surrounding the injection and arrival of targets at life fusion chamber center. *Fusion Sci Technol* 60: 61-65.
5. Kreutz RD (1988) Pellet Delivery for the Conceptual Inertial Confinement Fusion Reactor Hiball. *Fusion Technol* 8: 2708-

2720.

6. Aleksandrova IV, Koresheva ER, Koshelev EL (2022) A High-Pinning-Type-II Superconducting Maglev for ICF Target Delivery: main principles, material options and demonstration models. *High Power Lasers Sci Engin* 10: 1-9.
7. Antonov Yu F, Zaytcev AA (2017) Magnetolevitation transport technology. Moscow: FIZMATLIT, Russian Federation: 476.
8. Aleksandrova IV, Koresheva ER, Koshelev EL (2021) Target fabrication technologies and noncontact delivery systems to develop a free-standing target factory operating in the repetition mode at the IFE relevant level. *Nuclear Fusion* 61: 1-7.
9. Ginzburg VL, Andryushin EA (2004) Superconductivity. World Scientific Publishing Co, Revised edition: 106.
10. Landau LD, Lifshits EM (1982) Course of Theoretical Physics. Electrodynamics of continuous media. v.8, Moscow: Nauka, Russian Federation: 623.
11. Abrikosov AA (1957) About the magnetic properties of superconductors of the second group. *J Exp Theor Physics* 32: 1442-1452.
12. Haugan T, Barnes PN, Wheeler R, Meisenkothen F, Sumption M (2004) Addition of nanoparticle dispersions to enhance flux pinning of the YBa<sub>2</sub>Cu<sub>3</sub>O<sub>7-x</sub> superconductor. *Nature* 430: 867-870.
13. Taylan Koparan E, Surdu A, Kizilkaya K, Sidorenko A, Yanmaz E (2013) Pinning enhancement in MgB<sub>2</sub> superconducting thin films by magnetic nanoparticles of Fe<sub>2</sub>O<sub>3</sub>. *Bull Mater Sci*: 36: 961-966.
14. Jones A, Al-Qurainy M, Hamood AS, Lam SKH, Pan AV (2020) Dominant factors for the pinning enhancement by large artificial partial and complete antidots in superconducting films. *Supercond Sci Technol*: 33: 1-7.
15. Lee S, Petrykin V, Molodyk A, Samoilnikov S, Kaul A, et al. (2014) Development and production of second-generation high T<sub>c</sub> -superconducting tapes at SuperOx and first tests of model cables. *Supercond Sci Technol* 27: 1-9.
16. Gokhfeld DM, Koblishka MR, Koblishka-Veniova (2020) A. Highly porous superconductors: synthesis, research and prospects. *Physics of metals and metal science* 12: 1026-1038.

**Copyright:** ©2023 Elena Koresheva. This is an open-access article distributed under the terms of the Creative Commons Attribution License, which permits unrestricted use, distribution, and reproduction in any medium, provided the original author and source are credited.